IEEE Access
Multidisciplinary | Rapid Review | Open Access Journal

Received August 1, 2019, accepted August 18, 2019, date of publication August 22, 2019, date of current version September 10, 2019.

Digital Object Identifier 10.1109/ACCESS.2019.2936886

Articulated Laser Sensor for Three-Dimensional Precision Measurement

JIEHU KANG[1], BIN WU[1], AND TING XUE[2]
[1]State Key Laboratory of Precision Measuring Technology and Instruments, Tianjin University, Tianjin 300072, China
[2]School of Electrical and Information Engineering, Tianjin University, Tianjin 300072, China

Corresponding author: Bin Wu (wubin@tju.edu.cn)

This work was supported in part by the National Natural Science Foundation of China under Grant 61771336, and in part by the Natural Science Foundation of Tianjin in China under Grant 18JCZDJC38600.

ABSTRACT Breaking through the orthogonal shafting architecture of traditional measurement instruments, a novel articulated laser sensor for three-dimensional (3D) precision measurement is proposed. The novel sensor consists of two articulated laser sensing modules, and each module is mainly made up of two one-dimensional rotary tables and one collimated laser to achieve a flexible angle intersection. Moreover, a high-resolution digital camera is mounted on the right sensing module to achieve vision guidance. The three axes of each sensing module represent a non-orthogonal shafting architecture. The requirements of structural design, material selection, processing technology, assembling, calibration and maintain are greatly lowered. The costs are greatly reduced, including time and money. The system architecture, parameter calibration and measurement principle are elaborated. An accurate intersection model of two laser beams is proposed to calculate the accurate rotation angles of rotary tables by discrete point interpolation method. The experimental results showed that a maximum error less than 0.05 mm was detected from 100 mm to 500 mm. It is proved that 3D precision measurement is feasible with this proposed articulated laser sensor.

INDEX TERMS Articulated laser sensor, non-orthogonal shafting architecture, 3D precision measurement, accurate intersection model.

I. INTRODUCTION

Nowadays 3D precision measurement has been widely applied into many aspects, such as 3D shape detection, reverse modeling and quality control in manufacturing. The precision measurement instrument is a key part in the modern industry. It could greatly improve the automation level, and ensure the worker safety and product quality [1], [2].

3D vision sensors are widely applied in 3D measurement due to their characteristics of non-contact and abundant information. The common 3D vision sensors include stereo vision [3]–[7] and structured light vision [8]–[10]. The stereo vision systems require neither moving parts nor active illumination and provide high spatial resolution at low power consumption [11]. However, stereo vision has the disadvantages of large computation, poor match efficiency and poor robustness. Structured light vision system is an effective method to capture 3D information from the distorted images with the light patterns [12], [13]. By illuminating artificial pattern on the target object, it avoids the demand of natural texture on the object surface. Many companies such as Meta Vision, Servo Robot and Scout have developed various line structured light sensors. The laser structured light vision could only be applied into the local search and cannot provide global information about industrial environment [14].

Coordinate measuring machine (CMM) equipped with touch-trigger or scanning probes is a highly-accurate measurement instrument for 3D coordinates [15]–[17]. However, the widespread application of CMM is limited by its high cost and strict working condition. Theodolite and laser tracker [18]–[20] are widely employed for 3D measurement in industry owing to their highly-accurate. To achieve precision measurement, the three axes of theodolite and laser tracker are required to be strictly orthogonal. If the structural requirement cannot be achieved, the shafting tilt error will be produced. Therefore, the manufacturing and application costs are increased.

In the industrial applications, the interest is focused on their specific advantages when compared with other 3D measurement instruments, especially the cost and the compactness. There is increasing appreciation of the fact that 3D precision measurement in industrial applications will be low

The associate editor coordinating the review of this article and approving it for publication was Tao Liu.

cost, on-site and portable. For the deficiencies and application limitations of traditional measurement instruments, a novel articulated laser sensor is introduced for 3D precision measurement in this paper. The resulting sensor mainly consists of two articulated laser sensing modules which are based on non-orthogonal shafting architecture. As in traditional instruments, there are also three axes in each articulated laser sensing module, but with no the requirements of orthogonality and intersection.

The remainder of this paper is organized as follows. In Section II, the system architecture and measurement description of articulated laser sensor are introduced. In Section III, the parameters calibration method is presented. In Section IV, the mathematical model of the articulated laser sensor is set up in detail. In Section V, the accurate intersection model of two laser beams is introduced. In Section VI, the simulations based on Solidworks and actual measurement experiments are performed. Those simulation and experimental data validate that the proposed sensor is effective. The paper ends with some concluding remarks in Section VII.

II. SYSTEM ARCHITECTURE AND MEASUREMENT DESCRIPTION

A. NON-ORTHOGONAL SHAFTING ARCHITECTURE

To achieve precision measurement, traditional coordinate measurement instruments such as theodolite, total station and laser tracker require that the three axes are strictly orthogonal. The vertical axis is perpendicular to the horizontal axis and the horizontal axis is perpendicular to the measuring axis, as shown in Fig. 1. In addition, the three axes must intersect at one point, as shown in section view in Fig. 1. If the structural requirement of orthogonality has not been reached, the shafting tilt error will be generated. And the measurement accuracy of the instrument will be greatly reduced. The requirements of orthogonal shafting architecture are strict, including structural design, material selection, processing technology, assembling, calibration and maintain.

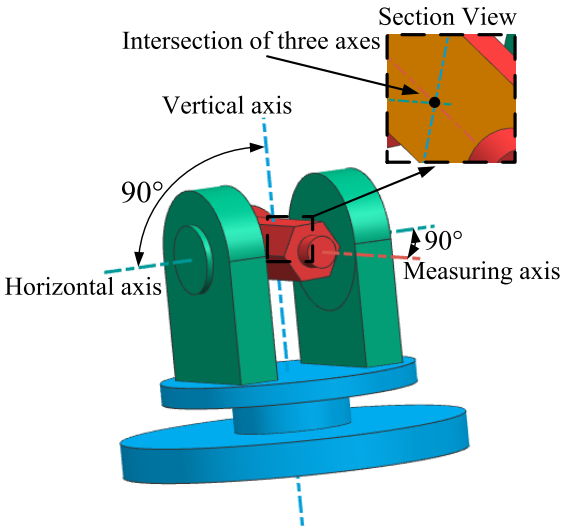

FIGURE 1. Structure diagram of orthogonal shafting architecture.

To reduce the manufacturing and application costs, a novel articulated laser sensing module is proposed. The novel sensing module mainly consists of two one-dimensional rotary tables and one collimated laser, as shown in Fig. 2. Compared with traditional orthogonal shafting instrument, the three axes of articulated laser sensing module represent a non-orthogonal shafting architecture without orthogonal and intersecting requirements. The three axes are 3D lines on different planes and the angle of accurate 90° between two axes is no longer needed. It means that the articulated laser sensing module can be quickly and easily built up with separate two rotary tables, one collimated laser and fixed connecting parts. The costs are greatly reduced, including time and money. In this paper, the dihedral angle of fixed connecting part is approximately 90° to expand the measurement space. Fortunately, the dihedral angle has no requirement of machining accuracy. To achieve different applications, the dihedral angle of fixed connecting part is variable.

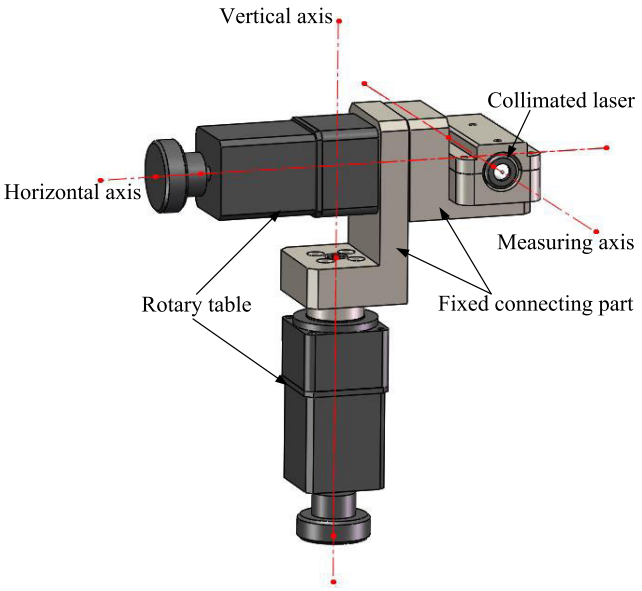

FIGURE 2. Structure diagram of non-orthogonal shafting architecture.

B. ARTICULATED LASER SENSOR

Two articulated laser sensing modules are combined into a novel articulated laser sensor to achieve 3D measurement, as shown in Fig. 3. In particular, a high-resolution digital camera is mounted on one sensing module to achieve vision guidance.

As with determining 3D coordinates utilizing traditional forward intersection measurement instruments, the articulated laser sensor operation is based on the intersection of two laser beams in the measuring zone. The coincidence of the two laser spots on the measured object denotes the intersection of the visualized measuring axes. As shown in Fig. 4,

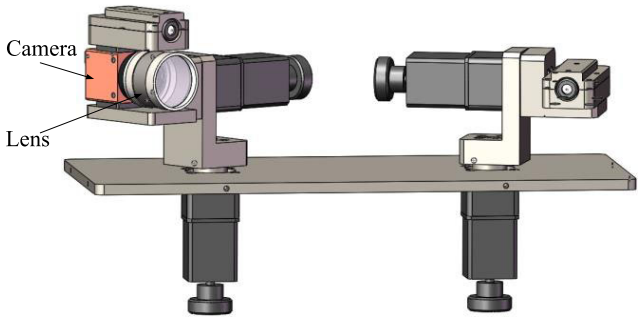

FIGURE 3. Structure diagram of articulated laser sensor.

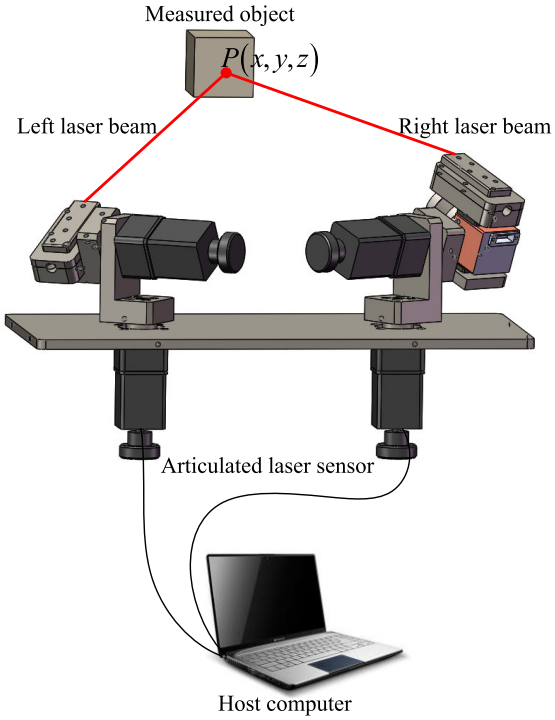

FIGURE 4. Structure diagram of the measurement system.

when the right laser beam intersects with the left laser beam on the measured object, the coordinate of a 3D point can be calculated based on the rotation angles provided by the rotary tables of two articulated laser sensing modules. The mathematical model will be introduced in Section IV and the accurate intersection model of two laser beams will be introduced in Section V.

III. PARAMETERS CALIBRATION

Calibrating the articulated laser sensor is a key aspect of 3D measurements, and the measurement accuracy depends heavily on the parameters calibration method [21], [22]. Obtaining the related position of three axes of articulated laser sensing module is needed. Three axes of each articulated laser sensing module can be described as three lines in 3D space, as shown in Fig. 5. The motion of measuring axis, which is a key part to receive the coordinates of measured points, could be

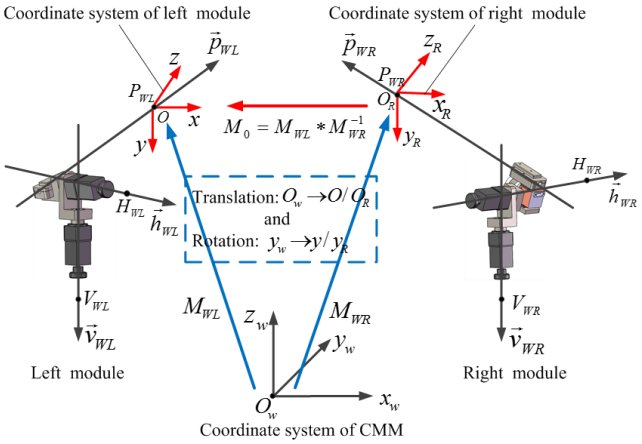

FIGURE 5. Schematic diagram of parameters calibration.

divided into two kinds of motion, including yawing rotation and pitching rotation. Yawing rotation is the rotating motion around vertical axis, and pitching rotation is the rotating motion around horizontal axis. To describe the movement of measuring axis, the spatial pose of each axis must be described, which is the so-called system parameters. The parameters of each axis consist of the direction vector and the fixed point on each axis, as shown in Fig. 5. The system parameters of the articulated laser sensor are listed in Table 1.

TABLE 1. The system parameters of articulated laser sensor.

Axis	Parameters
Vertical axis	Direction vector $\vec{v}_W = (x_{WV}, y_{WV}, z_{WV})$ Fixed point $V_W = (x_{WVO}, y_{WVO}, z_{WVO})$
Horizontal axis	Direction vector $\vec{h}_W = (x_{WH}, y_{WH}, z_{WH})$ Fixed point $H_W = (x_{WHO}, y_{WHO}, z_{WHO})$
Measuring axis	Direction vector $\vec{p}_W = (x_{WM}, y_{WM}, z_{WM})$ Fixed point $P_W = (x_{WMO}, y_{WMO}, z_{WMO})$

A. CALIBRATION OF VERTICAL AND HORIZONTAL AXES

A calibration method of articulated laser sensor has been proposed [23], which has been applied to this sensor successfully. To make precise measurements, it is necessary to calibrate the parameters with highly-accurate measurement instrument. A CMM is employed to calibrate articulated laser sensor in the laboratory. Two porcelain beads with highly-precision machining are adhered on the surfaces of two articulated laser sensing modules respectively, as shown in Fig. 6.

Rotating two articulated laser sensing modules vertically and horizontally every ten degrees and measuring the centers of beads in each position by CMM, thirty-six measured points are obtained from the complete trace of the beads.

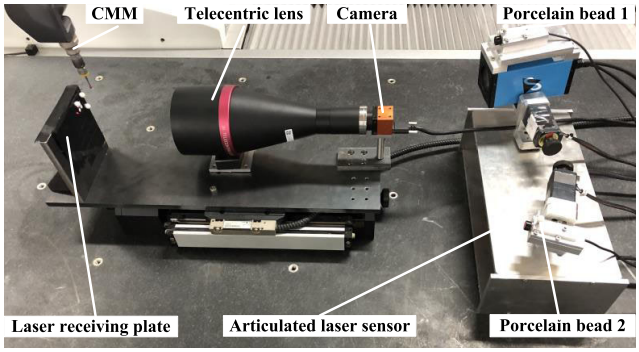

FIGURE 6. Overall setup of parameters calibration.

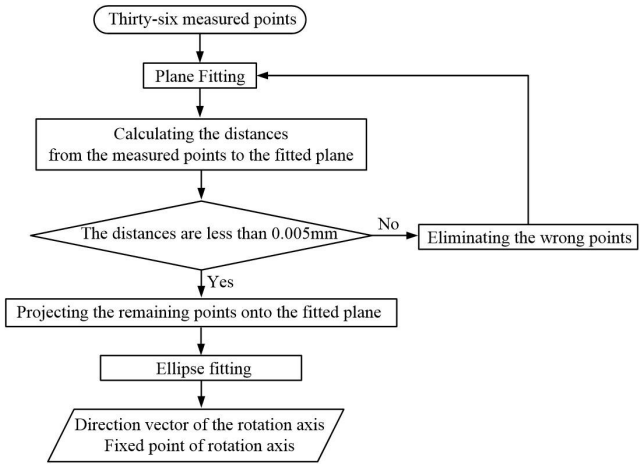

FIGURE 7. Flow chart of data processing of vertical and horizontal axes.

The parameters of horizontal axis and vertical axis are obtained by the least square method. The flow chart of data processing is shown in Fig. 7. The normal vector of fitted plane is recorded as the direction vector of the rotation axis, the ellipse center is recorded as the fixed point of each axis. Especially, the downward direction is taken as positive for the vertical axis.

B. CALIBRATION OF MEASURING AXIS

A laser receiving plate with high-precision machining is used to obtain the laser spot to calibrate the measuring axis, as shown in Fig. 6. Three porcelain beads are adhered on the surfaces of the laser receiving plate, which is improved to simplify the computing process compared with the method in reference [23]. The centers of beads are obtained by CMM and image processing, respectively. The centers of the laser spots on the image plane are obtained by image processing. By analysis of space vectors, the coordinates of laser spots on the laser receiving plate are obtained in CMM coordinate system. The flow chart of data processing is shown in Fig. 8.

Fortunately, the fixed points and direction vectors of three axes of two articulated laser sensing modules are described in CMM coordinate system. So the relative relationship of two articulated laser sensing modules can be obtained. Compared with traditional multi-station measurement system [24], a scale bar for calibrating the extrinsic parameters is no longer needed.

C. COORDINATE SYSTEM TRANSFORMATION IN CALIBRATION

The coordinate system of each articulated laser sensing module is defined as follows. As shown in Fig. 5, the coordinate systems of left and right module are transformed from CMM coordinate system, including one translation and one rotation. The origin of CMM coordinate system is translated to the fixed point on measuring axis, which is defined as the origin of coordinate system of each articulated laser sensing module. Then the y-axis of CMM coordinate system is rotated to be parallel to the direction vector of vertical axis, which is defined as the y-axis of coordinate system of each articulated laser sensing module. The translation is expressed by a translation vector T_W and the rotation is expressed by Rodrigues matrix R_W. The transformations from the CMM coordinate system to the coordinate system of left and right articulated laser sensing module is respectively expressed as

$$M_{WL} = \begin{bmatrix} R_{WL} & T_{WL} \\ 0 & 1 \end{bmatrix} \tag{1}$$

$$M_{WR} = \begin{bmatrix} R_{WR} & T_{WR} \\ 0 & 1 \end{bmatrix} \tag{2}$$

The transformations from the coordinate system of right articulated laser sensing module to left module is expressed as

$$M_0 = M_{WL} * M_{WR}^{-1} \tag{3}$$

IV. MATHEMATICAL MODEL

A. KINETIC MODEL OF ARTICULATED LASER SENSING MODULE

During measurement, the measuring axis is rotated around the vertical axis for yawing rotation and around the horizontal axis for pitching rotation. The transformation relationship of coordinate systems is shown in Fig. 9. The coordinate system of left articulated laser sensing module is defined as $Oxyz$ and set as the measurement coordinate system of articulated laser sensor. The coordinate system of right articulated laser sensing module is defined as $O_R x_R y_R z_R$.

To simplify the analysis, the left articulated laser sensing module is taken as an example. The right articulated laser sensing module is the same as left module. The fixed point on vertical axis is translated to the fixed point on measuring axis. So the vertical axis passes the origin of coordinate system of articulated laser sensing module, and the homogeneous translation vector is defined as T_{yaw}. The rotation matrix for yawing rotation is defined as R_{yaw}. The transformation matrix

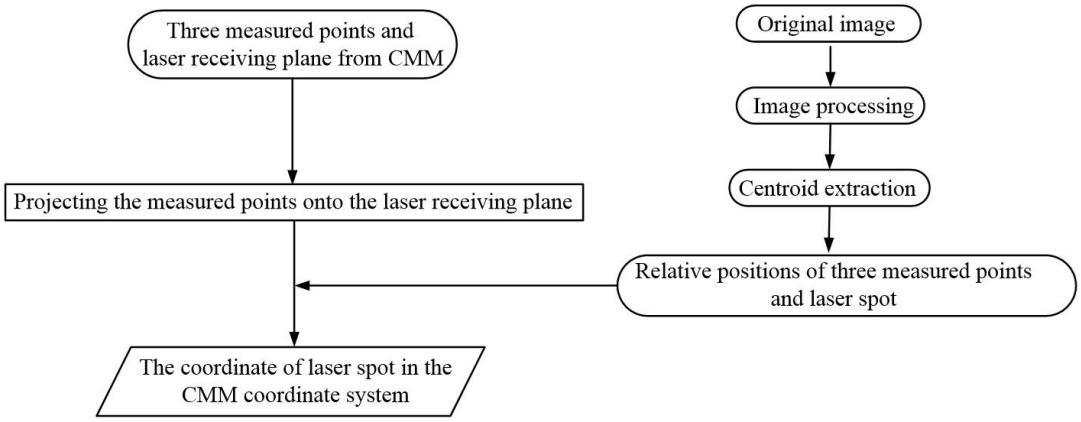

FIGURE 8. Flow chart of data processing of measuring axis.

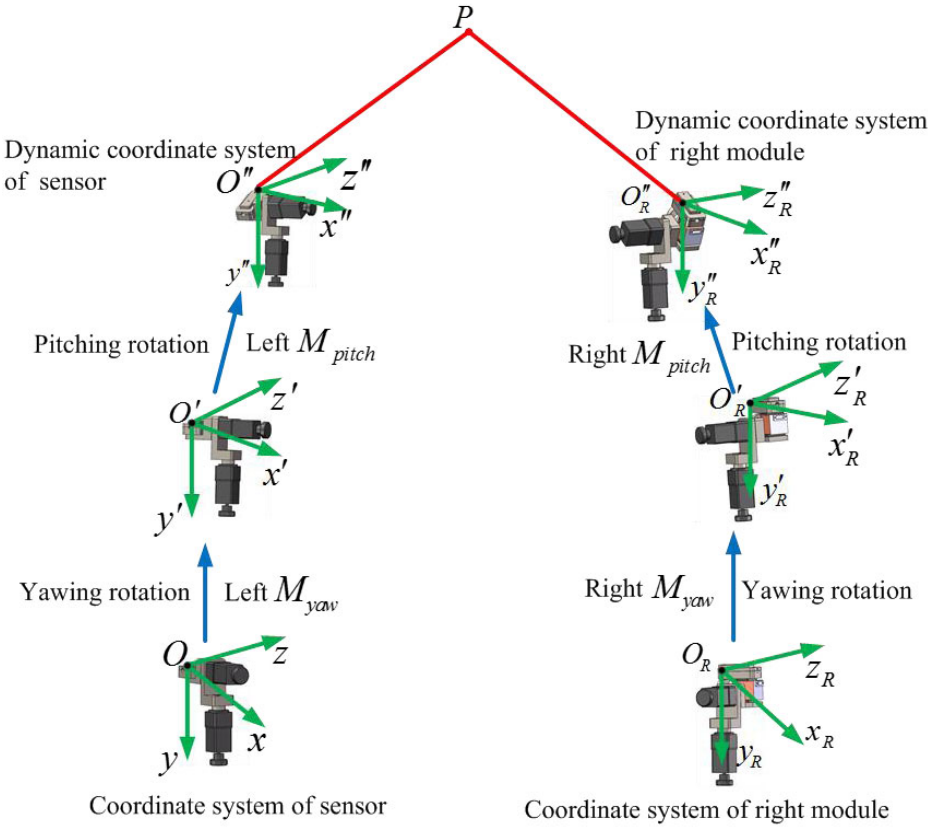

FIGURE 9. The transformation relationship of coordinate systems.

M_{yaw} of yawing rotation is described as

$$M_{yaw} = T_{yaw}^{-1} * R_{yaw}^{-1} * T_{yaw} \tag{4}$$

where $$R_{yaw} = \begin{bmatrix} \cos(\alpha) & 0 & \sin(\alpha) & 0 \\ 0 & 1 & 0 & 0 \\ -\sin(\alpha) & 0 & \cos(\alpha) & 0 \\ 0 & 0 & 0 & 1 \end{bmatrix}$$

and α represents the yawing rotation angle.

From the structure of articulated laser sensing module, the yawing rotation of horizontal axis is also described by M_{yaw}.

Then the pitching rotation is analyzed. The dynamic fixed point on horizontal axis is translated to the origin of dynamic coordinate system of articulated laser sensing module, and the homogeneous translation vector is defined as T_{pitch}. The rotation matrix for pitching rotation is defined as R_{pitch}. The transformation matrix M_{pitch} of pitching rotation is expressed

as

$$M_{pitch} = T_{pitch}^{-1} * R_{pitch} * T_{pitch} \tag{5}$$

where

$$R_{pitch} = \begin{bmatrix} q_0^2+q_1^2-q_2^2-q_3^2 & 2(q_1q_2-q_0q_3) & 2(q_1q_3+q_0q_2) & 0 \\ 2(q_1q_2+q_0q_3) & q_0^2-q_1^2+q_2^2-q_3^2 & 2(q_2q_3-q_0q_1) & 0 \\ 2(q_1q_3-q_0q_2) & 2(q_2q_3+q_0q_1) & q_0^2-q_1^2-q_2^2+q_3^2 & 0 \\ 0 & 0 & 0 & 1 \end{bmatrix}$$

and $q = q_0+q_1\cdot\vec{x}+q_2\cdot\vec{y}+q_3\cdot\vec{z} = \cos(\beta/2)+\vec{h}\cdot\sin(\beta/2)$ is a quaternion describing the rotation [25]. β represents the angle of pitching rotation and $\vec{h}$ is unit direction vector of dynamic horizontal axis, which is obtained by M_{yaw}.

Combining (4) and (5), the transformation matrix from initial coordinate system to dynamic coordinate system is described as

$$M_L = M_{pitch} * M_{yaw} \tag{6}$$

Similarly, the transformation matrix M_R of the right articulated laser sensing module is obtained.

B. THE CALCULATION MODEL OF SPATIAL COORDINATES

For the low-accuracy of traditional perspective projection model, the calculation model based on the midpoint of common perpendicular of lines on different planes is employed in this paper. The measuring axes of two articulated laser sensing modules are described as two lines on different planes, as shown in Fig. 10.

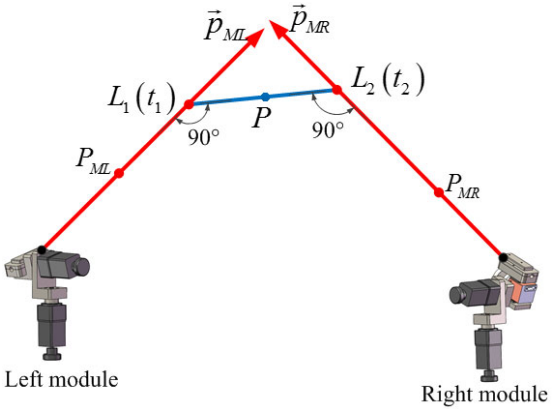

FIGURE 10. The calculation model of spatial coordinates.

Combining calibrated parameters and kinetic model, the direction vector and fixed point of measuring axis of left articulated laser sensing module are expressed as

$$\vec{p}_{ML} = M_L * M_{WL} * \vec{p}_{WL} \tag{7}$$

$$P_{ML} = M_L * M_{WL} * P_{WL} \tag{8}$$

where $\vec{p}_{WL}$ and P_{WL} have been obtained in Section III.

Similarly, the direction vector and fixed point of measuring axis of right module in coordinate system of sensor are expressed as

$$\vec{p}_{MR} = M_0 * M_R * M_{WR} * \vec{p}_{WR} \tag{9}$$

$$P_{MR} = M_0 * M_R * M_{WR} * P_{WR} \tag{10}$$

The measuring axes of two articulated laser sensing modules are respectively expressed as

$$L_1(t) = P_{ML} + t * \vec{p}_{ML} \tag{11}$$

$$L_2(t') = P_{MR} + t' * \vec{p}_{MR} \tag{12}$$

where t and t' represent length coefficients.

By setting $t = t_1$ and $t' = t_2$, two points of $L_1(t_1)$ and $L_2(t_2)$ are selected on two measuring axes, respectively. Assume that $L_1(t_1)$ and $L_2(t_2)$ are the foot points between two measuring axes and common perpendicular, as shown in Fig. 10. The dot product of $\vec{p}_{ML}$ and $\overrightarrow{L_1(t_1)L_2(t_2)}$ is 0 and the dot product of $\vec{p}_{MR}$ and $\overrightarrow{L_1(t_1)L_2(t_2)}$ is 0. t_1 and t_2 can be obtained by the following equations

$$\begin{cases} \vec{p}_{ML} \bullet \overrightarrow{L_1(t_1)L_2(t_2)} = 0 \\ \vec{p}_{MR} \bullet \overrightarrow{L_1(t_1)L_2(t_2)} = 0 \end{cases} \tag{13}$$

t_1 and t_2 are substituted into (11) and (12). And $L_1(t_1)$ and $L_2(t_2)$ are obtained.

The midpoint of common perpendicular is described as

$$P = [L_1(t_1) + L_2(t_2)]/2 \tag{14}$$

V. ACCURATE INTERSECTION MODEL

Accurate intersection of two laser beams is a crucial part to achieve precision measurement. For the limitation of angle resolution of rotary table, it is difficult to achieve accurate intersection. An accurate intersection model is proposed. The model is used to calculate the accurate rotation angles of rotary tables by discrete point interpolation method on non-accurate intersection conditions.

Each rotary table of the articulated laser sensing module is rotated in a small angle range. And the movement track AB of laser spot on the target plane is approximately a line, as shown in Fig. 11. The range of small angle is related to the measurement distance and the spatial positions of laser beam and target plane. Based on the pinhole camera model, $A'B'$ is the movement track of laser spot on the image plane. $A'B'$ is decomposed into two directions, u-axis and v-axis. The relationship between moving distance on each axis and the rotation angle of rotary table is approximately linear. The linear relationship is described as

$$\begin{cases} u = a_1\alpha + b_1\beta + c_1 \\ v = a_2\alpha + b_2\beta + c_2 \end{cases} \tag{15}$$

where (u, v) is the coordinate of laser spot on the image plane, (α, β) is the rotation angle of rotary table and (a_1, b_1, c_1) and (a_2, b_2, c_2) are the parameters of linear equations.

The rotary tables are rotated more than three times in a small angle range. And more than three sets of (u, v) and

TABLE 2. Comparison system parameters generated from Solidworks.

Axis	Left articulated laser sensing module (mm)	Right articulated laser sensing module (mm)
Vertical axis	Direction vector (0.147, 0.978, -0.147) Fixed point (-7.351, -48.907, 7.351)	Direction vector (0.147, 0.978, -0.147) Fixed point (214.298, -73.983, 62.165)
Horizontal axis	Direction vector (0.986, -0.157, 0.052) Fixed point (1.191, -94.362, 9.553)	Direction vector (0.969, -0.131, 0.212) Fixed point (223.378, -119.142, 66.868)
Measuring axis	Direction vector (0.017, 0.330, 0.944) Fixed point (6.149, -91.682, 5.607)	Direction vector (-0.141, 0.351, 0.926) Fixed point (229.172, -119.415, 63.811)

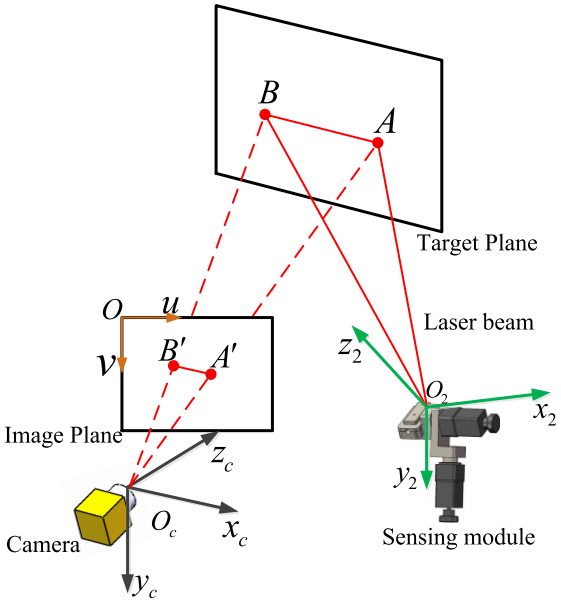

FIGURE 11. Schematic diagram of accurate intersection.

(α, β) are obtained. (a_1, b_1, c_1) and (a_2, b_2, c_2) are derived by least square method as follows

$$\begin{cases} L_1 = \left(A^T A\right)^{-1} A^T U \\ L_2 = \left(A^T A\right)^{-1} A^T V \end{cases} \tag{16}$$

where $L_1 = [a_1, b_1, c_1]^T$, $L_2 = [a_2, b_2, c_2]^T$, $U = [u_1, u_2, u_3 \cdots u_n]^T$,

$$V = [v_1, v_2, v_3 \cdots v_n]^T, \quad A = \begin{bmatrix} x_1 & y_1 & 1 \\ x_1 & y_1 & 1 \\ \cdots & \cdots & \cdots \\ x_n & y_n & 1 \end{bmatrix}.$$

Combining (15) and (16), the matrix equation is obtained

$$\begin{bmatrix} \alpha \\ \beta \\ 1 \end{bmatrix} = \left(\begin{bmatrix} a_1 & b_1 & c_1 \\ a_2 & b_2 & c_2 \\ 0 & 0 & 1 \end{bmatrix}^{-1} \right) \begin{bmatrix} u \\ v \\ 1 \end{bmatrix} \tag{17}$$

The left laser spot coordinate of (u_0, v_0) on the image plane is substituted into (17). And the rotation angles of right sensing module are obtained, which are corresponding to the accurate intersection of two laser beams.

VI. VALIDATION EXPERIMENTS

A. SIMULATION OF ARTICULATED LASER SENSOR MEASUREMENT

Based on Solidworks, a simulation environment for articulated laser sensor is set up as shown in Fig. 12. The measurement distance for simulation is from 100 mm to 500 mm. 65 points are placed in different positions in the measurement space. The system parameters of articulated laser sensor are calibrated in the Solidworks coordinate system, as shown in Table 2. Corresponding to the practical calibration, the value of calibrated parameters are accounted to three decimal places.

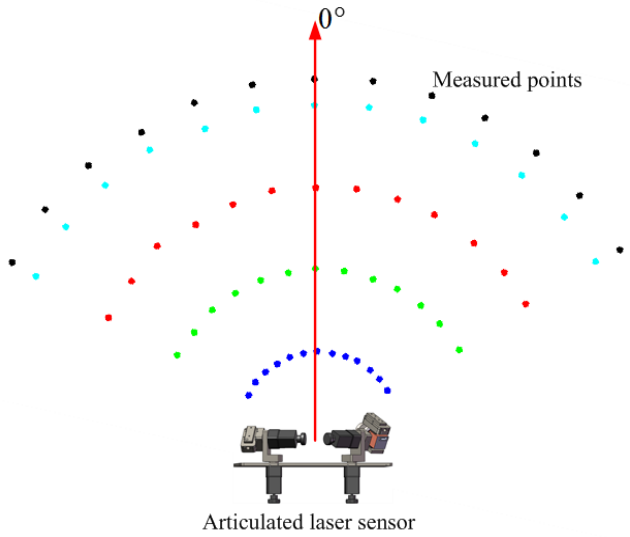

FIGURE 12. Schematic diagram of simulation environment.

Utilizing the simulation system parameters of the articulated laser sensor, the 3D coordinates of the remaining 65 points were obtained. The truth 3D coordinates are generated by Solidworks. The deviations of measured values and truth values are shown in Fig. 13 and Table 3.

Combining Fig. 12, Fig. 13 and Table 3, the simulation results are obtained as follows. First, the articulated laser sensor is able to deliver a high performance and the maximum measurement error is less than 0.02 mm from 100 mm to 500 mm in the simulation environment, which is generated

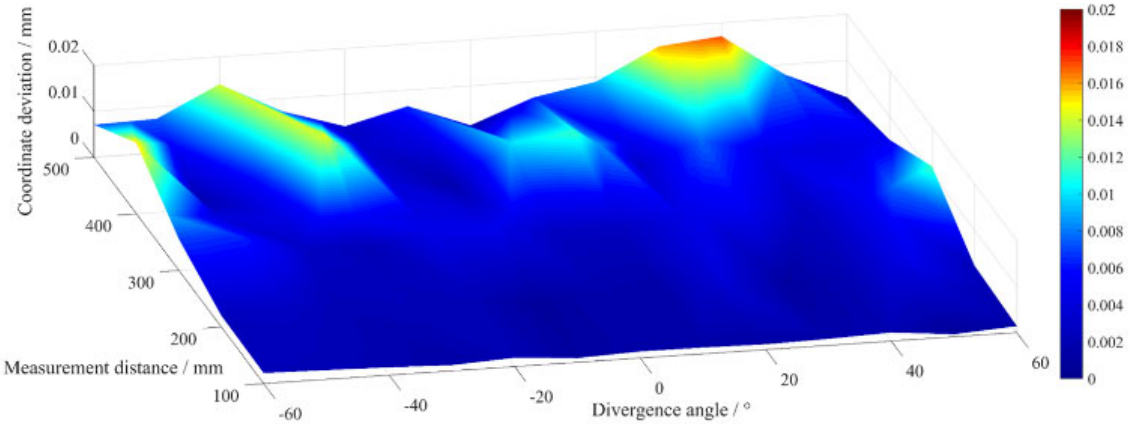

FIGURE 13. The deviations of measured values and truth values.

TABLE 3. comparison between measured values and truth values in simulation.

Max deviation (mm)	Min deviation (mm)	Average (mm)	Std. deviation (mm)
0.017	0.001	0.005	0.004

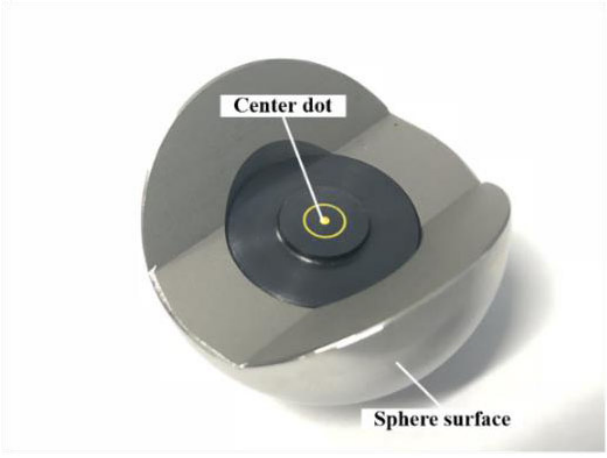

FIGURE 14. High-precision machining hemispherical target.

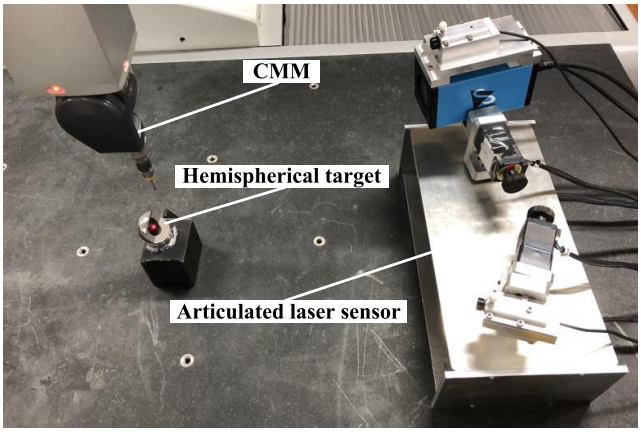

FIGURE 15. Overall experimental setup of articulated laser sensor.

from the rounding error of decimal places. Second, the measurement error increases with the increase of measurement distance. Third, the measurement error approximatively increases with the increase of the divergence angle, whose zero reference is shown in Fig. 12.

B. EXPERIMENTS OF ARTICULATED LASER SENSOR MEASUREMENT

In the experiment, a CMM was employed to calibrate the system parameters. By measuring the small adhered balls rotated around the corresponding axes, the direction vectors and fixed points of the horizontal and vertical axes were obtained by ellipse fitting. And the spatial position of measuring axis could be obtained by the CMM and image processing. The system parameters in the CMM coordinate system are shown in Table 4.

To obtain an extremely highly-accurate spatial coordinate of the intersection of two laser beams, a high-precision machining hemispherical target with the centre dot is employed, as shown in Fig. 14. The coordinate of centre dot are obtained by two measuring ways, as shown in Fig. 15. The points on the sphere surface are measured by CMM and the coordinate of centre dot is received by sphere surface fitting, which is defined as reference value. The intersection of two laser beams is measured by articulated laser sensor, which is defined as measured value. 20 measured points are placed in different positions in the measurement space, as shown in Fig. 16. The deviations of measured values and reference values are shown in Fig. 17 and Table 5.

From the Fig. 16, Fig. 17 and Table 5, the experimental results are obtained as follows. First, the maximum measurement error is less than 0.05 mm from 100 mm to 500 mm in the real experimental, which is worse than the simulation results. Second, the overall trend of the measurement error is the same as the simulation results.

TABLE 4. The intrinsic parameters calibrated by CMM.

Axis	Left articulated laser sensing module (mm)	Right articulated laser sensing module (mm)
Vertical axis	Direction vector (0.001802, 0.004509, -0.999988) Fixed point (212.588, 49.535, -604.122)	Direction vector (-0.005815, 0.004339, -0.999974) Fixed point (373.639, 50.427, -525.154)
Horizontal axis	Direction vector (0.974637, -0.223787, 0.001371) Fixed point (163.701, 60.892, -621.959)	Direction vector (0.986801, 0.161851, -0.005349) Fixed point (439.757, 61.650, -622.794)
Measuring axis	Direction vector (0.221297, 0.974611, 0.034063) Fixed point (311.598, 711.725, -596.611)	Direction vector (-0.198316, 0.974778, -0.102368) Fixed point (317.737, 672.093, -596.205)

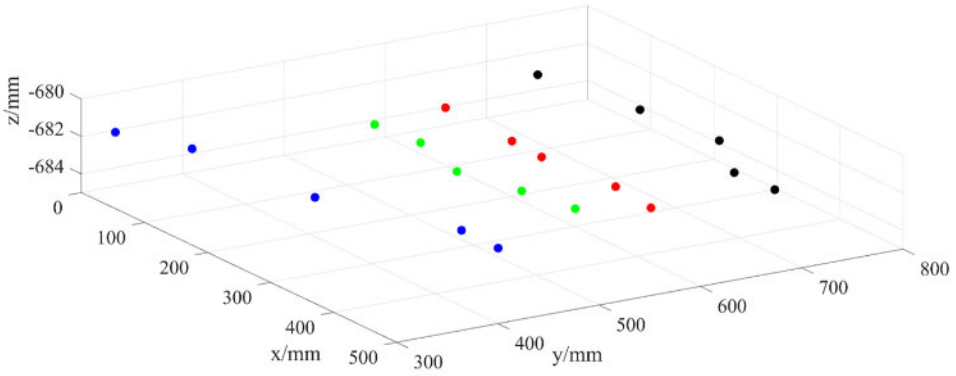

FIGURE 16. Schematic diagram of the measured points.

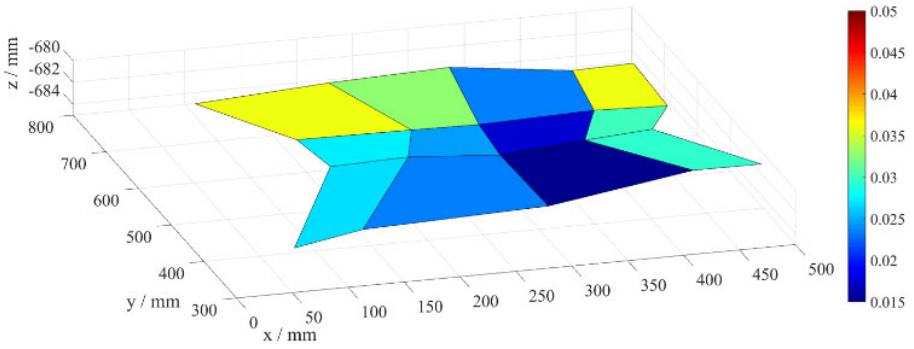

FIGURE 17. The deviations of measured values and reference values.

TABLE 5. Comparison between measured value and reference value in experiment.

Max deviation (mm)	Min deviation (mm)	Average (mm)	Std. deviation (mm)
0.048	0.015	0.033	0.009

VII. CONCLUSION AND FUTURE WORK

A. CONCLUSION

Based on non-orthogonal shafting architecture, a novel articulated laser sensor for 3D precision measurement is proposed in this paper. The presented sensor mainly consists of four one-dimensional rotary tables, two collimated laser and one camera. Although the uncertainty of assemblage, the system parameters of sensor are calibrated accurately by CMM and image processing. The measurement principle is elaborated. The experimental results show that the maximum measurement error of the proposed sensor is less than 0.05 mm. The encouraging results prove that this sensor is suitable for 3D measurement applications.

B. FUTURE WORK

Motivated by the increasing demands in the industrial applications, the measurement distance will be expanded to 1000 mm and measurement accuracy will be improved in the

following work. However, the measurement error increases with the increase of measurement distance. It is necessary to carry out uncertainty evaluation and error compensation.

The studies of the non-orthogonal shafting architecture are important to theoretical research and practical application. This architecture can be easily transplanted for different applications. By changing the type, number and layout of rotary tables and laser, the different measurement distances and accuracies can be realized. For instance, the distance of two non-orthogonal module is enlarged to achieve the large-scale measurement. The non-orthogonal shafting architecture is expected to develop a novel precision measurement method and a series of novel precision measurement instruments.

REFERENCES

[1] L. Yang, E. Li, T. Long, J. Fan, and Z. Liang, "A high-speed seam extraction method based on the novel structured-light sensor for arc welding robot: A review," *IEEE Sensors J.*, vol. 18, no. 21, pp. 8631–8641, Nov. 2018.
[2] M. Ramakrishnan, G. Rajan, Y. Semenova, D. Callaghan, and G. Farrell, "Investigation of the effect of vibration amplitude on vibration measurements of polarimetric fiber sensors embedded in composite beams," *Smart Mater. Struct.*, vol. 23, no. 4, Mar. 2014, Art. no. 045037.
[3] D. Bračun and A. Sluga, "Stereo vision based measuring system for online welding path inspection," *J. Mater. Process. Technol.*, vol. 223, pp. 328–336, Sep. 2015.
[4] Y. Xu, H. Yu, J. Zhong, T. Lin, and S. Chen, "Real-time seam tracking control technology during welding robot GTAW process based on passive vision sensor," *J. Mater. Process. Technol.*, vol. 212, no. 8, pp. 1654–1662, Aug. 2012.
[5] Y. Zou, X. Chen, G. Gong, and J. Li, "A seam tracking system based on a laser vision sensor," *Measurement*, vol. 127, pp. 489–500, Oct. 2018.
[6] F. Zhou, B. Peng, Y. Cui, Y. Wang, and H. Tan, "A novel laser vision sensor for omnidirectional 3D measurement," *Opt. Laser Technol.*, vol. 45, pp. 1–12, Feb. 2013.
[7] H. Xie, A. Jiang, H. A. Wurdemann, H. Liu, L. D. Seneviratne, and K. Althoefer, "Magnetic resonance-compatible tactile force sensor using fiber optics and vision sensor," *IEEE Sensors J.*, vol. 14, no. 3, pp. 829–838, Mar. 2014.
[8] X. Gao, D. You, and S. Katayama, "Seam tracking monitoring based on adaptive Kalman filter embedded Elman neural network during high-power fiber laser welding," *IEEE Trans. Ind. Electron.*, vol. 59, no. 11, pp. 4315–4325, Nov. 2012.
[9] B. Wu, T. Xue, T. Zhang, and S. Ye, "A novel method for round steel measurement with a multi-line structured light vision sensor," *Meas. Sci. Technol.*, vol. 21, no. 2, Feb. 2010, Art. no. 025204.
[10] E. Lilienblum and A. Al-Hamadi, "A structured light approach for 3-D surface reconstruction with a stereo line-scan system," *IEEE Trans. Instrum. Meas.*, vol. 64, no. 5, pp. 1258–1266, May 2015.
[11] T. F. Comas, C. Diao, J. Ding, S. Williams, and Y. Zhao, "A passive imaging system for geometry measurement for the plasma Arc welding process," *IEEE Trans. Ind. Electron.*, vol. 64, no. 9, pp. 7201–7209, Sep. 2017.
[12] J. Salvi, J. Pagès, and J. Batlle, "Pattern codification strategies in structured light systems," *Pattern Recognit.*, vol. 37, no. 4, pp. 827–849, Apr. 2004.
[13] L. Yang, E. Li, T. Long, J. Fan, and Z. Liang, "A novel 3-D path extraction method for arc welding robot based on stereo structured light sensor," *IEEE Sensors J.*, vol. 19, no. 2, pp. 763–773, Jan. 2018.
[14] Z. Song and R. Chung, "Determining both surface position and orientation in structured-light-based sensing," *IEEE Trans. Pattern Anal. Mach. Intell.*, vol. 32, no. 10, pp. 1770–1780, Oct. 2010.
[15] E. Savio, L. D. Chiffre, and R. Schmitt, "Metrology of freeform shaped parts," *Ann.-Manuf. Technol.*, vol. 56, pp. 810–835, Apr. 2007.
[16] H. Hansen, K. Carneiro, H. Haitjema, and L. Chiffre, "Dimensional micro and nano metrology," *Ann.-Manuf. Technol.*, vol. 55, pp. 721–743, Sep. 2006.
[17] M. Ren, L. Kong, L. Sun, and C. Cheung, "A curve network sampling strategy for measurement of freeform surfaces on coordinate measuring machines," *IEEE Trans. Instrum. Meas.*, vol. 66, no. 11, pp. 3032–3043, Nov. 2017.
[18] S. Aguado, J. Santolaria, D. Samper, and J. J. Aguilar, "Forecasting method in multilateration accuracy based on laser tracker measurement," *Meas. Sci. Technol.*, vol. 28, no. 2, Feb. 2017, Art. no. 025011.
[19] R. Summan, S. G. Pierce, C. N. Macleod, G. Dobie, T. Gears, W. Lester, P. Pritchett, and P. Smyth, "Spatial calibration of large volume photogrammetry based metrology systems," *Measurement*, vol. 68, pp. 189–200, May 2015.
[20] H. Jing, C. King, and D. Walker, "Measurement of influence function using swing arm profilometer and laser tracker," *Opt. Express*, vol. 18, no. 5, pp. 5271–5281, Mar. 2010.
[21] D. Wu, T. Chen, and A. Li, "A high precision approach to calibrate a structured light vision sensor in a robot-based three-dimensional measurement system," *Sensors*, vol. 16, no. 9, p. 1388, Sep. 2016.
[22] S. Yin, Y. Ren, Y. Guo, J. Zhu, S. Yang, and S. Ye, "Development and calibration of an integrated 3D scanning system for high-accuracy large-scale metrology," *Measurement*, vol. 54, pp. 65–76, Aug. 2014.
[23] J. Kang, B. Wu, X. Duan, and T. Xue, "A novel calibration method of articulated laser sensor for trans-scale 3D measurement," *Sensors*, vol. 19, no. 5, p. 1083, 2019.
[24] B. Wu, F. Yang, W. Ding, and T. Xue, "A novel calibration method for non-orthogonal shaft laser theodolite measurement system," *Rev. Sci. Instrum.*, vol. 87, no. 3, Feb. 2016, Art. no. 035102.
[25] X. Xu, X. Tian, and L. Zhou, "A robust incremental-quaternion-based angle and axis estimation algorithm of a single-axis rotation using MARG sensors," *IEEE Access*, vol. 6, pp. 42605–42615, 2018.
[26] G. Wang, X. Liu, and S. Han, "A method of robot base frame calibration by using dual quaternion algebra," *IEEE Access*, vol. 6, pp. 74865–74873, 2018.

JIEHU KANG received the B.S. degree in measurement and control technology and instrument and the M.S. degree in instrumentation science and technology from Tianjin University, Tianjin, China, in 2010 and 2013, respectively, where he is currently pursuing the Ph.D. degree in instrumentation science and technology. His research interests include precision measurement technology and instruments, laser and vision measurement technology, and smart sensors.

BIN WU received the B.S. degree in measurement and control technology and instrument and the Ph.D. degree in measurement technology and instruments from Tianjin University, Tianjin, China, in 1997 and 2002, respectively, where he is currently a Professor with the Department of Instrumentation Science and Technology. His research interests include laser and photoelectric testing technology, precision measurement technology and instruments, and vision measurement technology.

TING XUE received the B.S., M.S., and Ph.D. degrees from the College of Precision Instrument and Optoelectronics Engineering, Tianjin University, Tianjin, China, in 1998, 2004, and 2007, respectively, where she is currently an Associate Professor with the College of Electrical Engineering and Automation. Her current research interests include multiphase flow measurement, vision inspection, and opto-electrical systems.